SAJSET
ISSN: 2992-3581

Savannah Journal of Science and Engineering Technology
Volume: 02; Issue: 05; Pages: 203-213; 2024.
www.sajsetjournal.com.ng

DOI: xx.xxxx.x/sajset-02-2024-0028

SAJSET
ISSN: 2992-3581

Optimizing PV power production by incremental conductance and model predictive control maximum power point tracking technique

[1]Jada, A. M., [2,3]Abdulkarim, A., [2,4]Mohammed, M., [2]Seidu, I. and [2]Aliyu, A. J.
[1]*Department of Electrical Engineering, Adamawa State Polytechnic, Yola*
[2]*Department of Electrical Engineering, Ahmadu Bello University, Zaria*
[3]*Department of Electrical and Telecommunications Engineering, Kampala International University, Kansanga, Kampala*
[4]*Kaduna State Power Supply Company (KAPSCO), Kaduna*

Paper History
Received: 01st August, 2024
Accepted: 26th August, 2024
Published: Sept., 2024

Corresponding author
Jada, A. M.
mabduljada@gmail.com

Abstract:
Photovoltaic (PV) energy sources play a crucial role in renewable energy applications, but their energy conversion efficiency remains relatively low. Despite the vital role played by Maximum Power Point Tracking (MPPT) algorithms for optimizing power production from PV systems, they are associated with delay in response time, which potentially leads to insufficient energy harvesting. Addressing this challenge requires collaborative efforts from researchers. This study improved the dynamic capability of maximum power tracking technique by combining Incremental Conductance (INC) MPPT algorithm and Model Predictive Control (MPC) algorithm. The improved method has achieved a tracking efficiency of 98.2% at 25^{0}C, 98.8% at 35^{0}C and 98.5% at 25^{0}C under varying temperature and constant irradiance condition of 1000W/m^2.This indicate that the developed method is more effective in optimizing the MPPT technique. When compared with Perturb and Observe-MPC method, the developed method has a faster dynamic capability, better tracking performance and is more effective in maximizing the power output of PV system.

Keywords: *Conductance, Energy, Photovoltaic, Power tracking, Predictive Control, Solar*

1. Introduction

Solar power generation involves harnessing electricity from solar energy, which is the radiant energy emitted by the sun in the form of heat and light. This process utilizes two primary methods: solar photovoltaic (PV) and solar thermal power generation. In solar thermal power, sunlight is used to generate heat that is transferred to a fluid. This fluid then transforms the heat energy into steam, propelling a turbine connected to a generator and thereby producing electricity [1]. In solar PV power generation, sunlight is directly converted into electricity through modules comprising numerous PV cells [2]. Solar energy represents eco-friendly technology, offering a robust energy source and standing as one of the foremost renewable and environmentally conscious energy sources. It holds a pivotal role in realizing sustainable energy solutions for development. The substantial daily availability of solar energy makes it an exceptionally appealing resource for electricity generation. Both concentrated solar power and solar PV continue to undergo continuous advancements to meet our evolving energy requirements [3]. Solar power resources are widely utilized in renewable energy applications [4], PV energy sources exhibit an energy conversion efficiency that is still considered relatively low. In PV systems, utilization of Maximum Power Point Tracking (MPPT) algorithm is crucial to optimize energy generation. The Perturb and Observe, as well as INC methods are acknowledged and frequently favored among the various MPPT algorithms [4]. Studies indicate that INC outperforms Perturb & Observe, especially in rapidly changing weather conditions, boasting superior noise rejection and reduced confusion from system dynamics [5].

The rapid adaptability of MPPT algorithms becomes crucial when faced with sudden changes in the system, such as partial shading effects [6]. Literatures has introduced various strategies to enhance response times in such scenarios, including genetic algorithms, sliding mode, fuzzy logic, Model Predictive Control (MPC) and Artificial Neural Networks (ANN) [7 - 11]. These methods often demand substantial computational power for swift dynamic responses. MPC, as a contemporary alternative, has bolstered digital hardware processing capabilities [12]. Apart from delivering rapid dynamic responses and precise control, MPC boasts benefits like seamless adaptation to multivariable cases, integration of non-linearity, straightforward controller implementation, and a flexible structure for application of specific modifications and extensions [12]. Applications of MPC in power converters, particularly in boost converters for voltage control, reveal minimal overshooting during voltage control processes [13]. Comparative analyses consistently favor MPC over

conventional methods [14, 15], while hybrid control methods combining MPC with other algorithms enhance sensitivity [8, 16]. For this reason, various algorithms are combined with the MPPT algorithm, using current or voltage values at the MPP as references for MPC [17]. Although hybrid algorithms outperform classical ones in control capabilities, some studies highlight delayed response times as a drawback [18]. To mitigate this, a model-based MPPT and ANN techniques has been proposed, resulting in enhanced dynamic response and reduced transition times [6]. Another study successfully combined MPC and P&O MPPT techniques, effectively reducing dynamic response times under variable irradiance conditions [13, 19].

So, the effectiveness of a PV system depends on configuration of PV panels, the efficiency of DC-DC converters, and the performance of the MPPT technique [20]. While boosting the efficiency of PV modules requires costly advanced fabrication technology, current efforts are directed towards enhancing other components of the system. Given these considerations, the objective of this research is to improve the dynamic capability of the control methodology by using INC MPPT algorithm with the MPC algorithm.

2. Methodology

This study utilized a boost converter configuration connected to PV module outputs to facilitate power flow control. Figure 1 depicts the schematic overview of the entire system. On the control aspect, an INC MPPT algorithm is implemented to obtain the voltage at the Maximum Power Point (MPP). This value serves as a reference in the MPC algorithm responsible for regulating the input current of the converter. The MPC algorithm generates suitable switching signals to align the inductor current with the reference value.

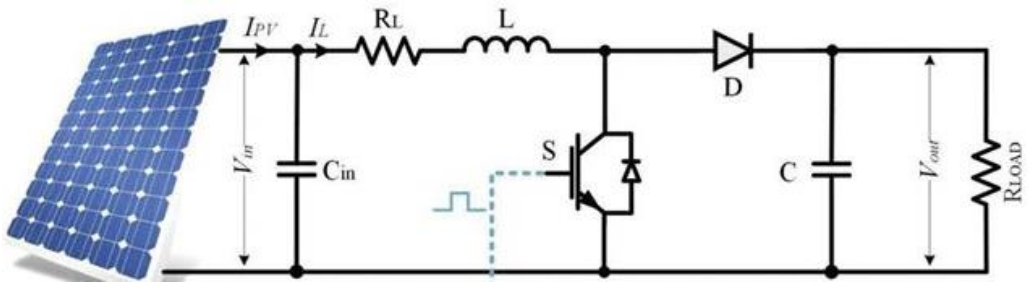

Figure 1: Schematic Diagram for INC-MPC

2.1 Mathematical formulation of solar PV module

The fundamental building block of PV system is PV cell. By interconnecting multiple PV cells, a PV module is formed, and combining several modules results in the creation of a panel [21]. When these panels are assembled, they collectively form a PV array, which comprises diverse PV cells connected through both series and parallel configurations. The series connections serve to boost voltage of the system, whereas the parallel connections enhance current within the module. The PV system's electricity generation hinges on both solar temperature and intensity of irradiation. In a standard electrical circuit model for a solar cell, you have a photo-generated current (I_{pg}), a shunt resistor (R_{shunt}), an inverted diode, and a resistor in series (R_s) accounting for internal losses from current flow, as illustrated in Figure 2. The mathematical representation for the current of a PV cell is shown in equations 1 to 3 [21]

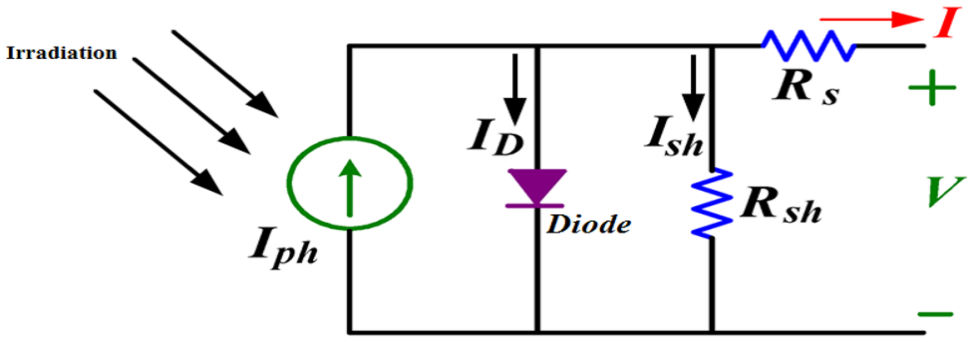

Figure 2: Realistic circuit of a PV cell [21]

$$I_{pv} = I_{pg} - I_{Diode} - I_{Shunt} \quad (1)$$

Where I_{pv} represent the current of a PV cell (A), I_{pg} denote photo-generated current (A), I_{Diode} stand for the diode current (A), and I_{Shunt} represent shunt current (A).

According to equation of Shockley diode, current through the diode can be expressed as in equation 2 [2]:

$$I_{Diode} = I_{ox}\left(exp\left[\frac{q_e(V_{pv}+IR_s)}{m_d k_g T_c}\right] - 1\right) \quad (2)$$

As per the model, the mathematical representation for current in a PV cell is articulated in equation 3 [21]:

$$I_{pv} = I_{pg} - I_{ox}\left(\exp\left[\frac{q(V_{pv}+IR_s)}{m_d k_g T_c}\right] - 1\right) - \frac{(V+IR_s)}{R_{shunt}} \quad (3)$$

Where I_{ox} denotes diode saturation current (A), q_e is elementary charge. K_g is Boltzmann gas constant. m_d is quality factor of the diode, V_{pv} is voltage of the PV cell, T_c is cell temperature, R_s is series resistance and R_{shunt} is shunt resistance

The single and double diodes models are main models utilized in PV modules. Despite the enhanced accuracy offered by the double diode model, single diode model is often preferred due to its simplicity [21]:

The MPP (I_{mpp})'s current can be represented as shown in equation 4 [21]:

$$I_{mpp=} I_{pg} - I_{ox}\left(exp\left[\frac{q_e(V_{mpp}+I_{mpp}R_s)}{m_d k_g T_c}\right] - 1\right) - \frac{(V_{mpp}+I_{mpp}R_s)}{R_{shunt}} \quad (4)$$

Hence, the expression for the MPP(P_{mpp}) power can be represented as shown in equation 5:

$$P_{mpp=} V_{mpp}\left\{I_{pg} - I_{ox}\left(exp\left[\frac{q_e(V_{mpp}+I_{mpp}R_s)}{m_d k_g T_c}\right] - 1\right) - \frac{(V_{mpp}+I_{mpp}R_s)}{R_{shunt}}\right\} \quad (5)$$

2.2 Modeling of Boost Converter

DC–DC converters are modeled under various operational scenarios, including Continuous Conduction Mode (CCM) and Discontinuous Conduction Mode (DCM) with careful consideration given to factors such as potential switching states, switching frequency, input voltage, and passive components of the converter. Depending on the system parameters under investigation, the control methodology for the converter is utilized for CCM conditions [4].

The analysis of the converter encompasses two primary states of the switch, delineated in Figure 3 and Figure 4 respectively. During the ON state of the switch, the calculation of inductor current (I_L) is facilitated by equation 6. Conversely, Figure 4 illustrates the circuit model during the OFF state of the switch, where the load is powered by both the inductor and the input source. As a result, the input current can be determined utilizing equation 7 [4].

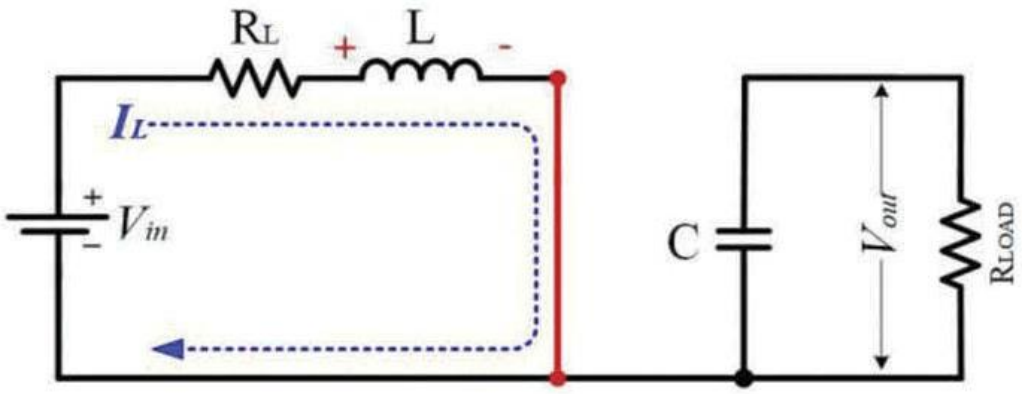

Figure 3: Converter Circuit Diagram when the switch is ON [4]

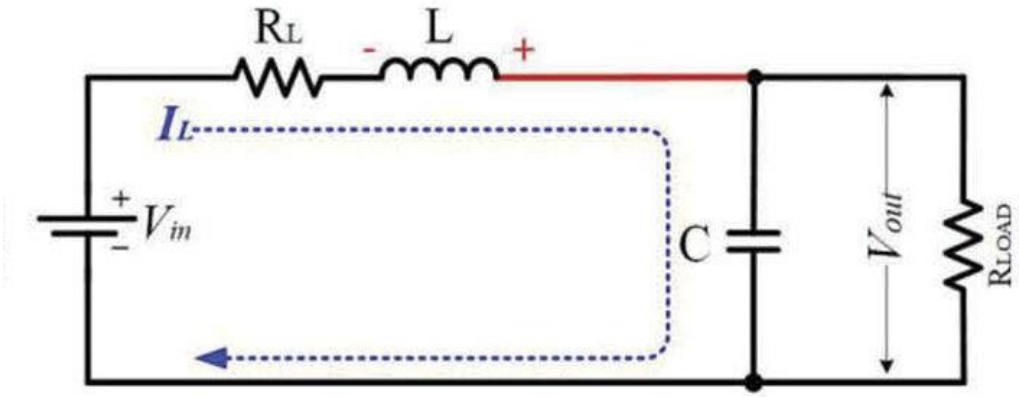

Figure 4: Converter Circuit Diagram when the switch is OFF [4]

$$\frac{dV_L}{dt} = -\frac{R_L(V_{in}-I_L R_L)}{L} \quad (6)$$

$$\frac{dV_L}{dt} = -\frac{R_L(V_{in}-I_L R_L-V_{out})}{L} \quad (7)$$

Where L represents inductance, R_L stand for resistance value, v_{in} for input voltage, V_{out} output voltage and I_L stand for Inductor current.

Voltage during switching period can be obtain by combining equations 6 and 7

$$\frac{dV_L}{dt} = -\frac{R_L(V_{in}-I_L R_L-V_{out}(1-d))}{L} \quad (8)$$

Where *d* is equal to 0 for OFF position of switch, and 1 for ON

2.3 INC MPPT algorithm

INC Peak Power Point Tracking Algorithm is a commonly employed method in PV systems intended to improve the power of solar panels. The core principle of the INC algorithm is grounded in the notion that at the maximum power point, the derivative of power with respect to voltage (ΔP/ΔV) is zero [21]. The INC algorithm has two essential sensors, the voltage sensor and the current sensor. These sensors are necessary for measuring both the output voltage and current of the PV device. The implementation flowchart for INC algorithm is depicted in Figure 5 [22].

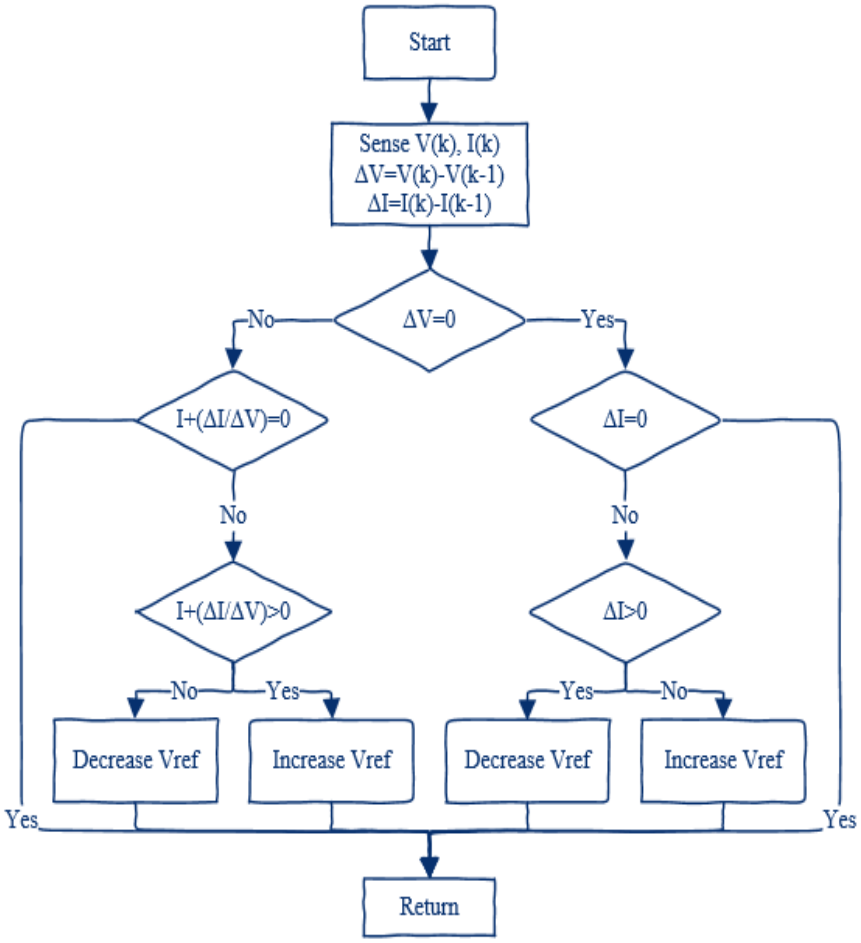

Figure 5: Flowchart for Incremental Conductance algorithm [22]

$$P = VI \quad (9)$$

This algorithm can be expressed mathematically, as demonstrated by Mohamed and Abd-El-Sattar [21] and the power generated from the source (P) can be depicted as illustrated in equation 10:

$$P_{pv} = V_{pv}I_{pv} \quad (10)$$

With the relationship $P_{pv} = V_{pv}I_{pv}$ and applying the chain rule, the result is as follows:

$$\frac{dP_{pv}}{dV_{pv}} = \frac{d(V_{pv}I_{pv})}{dV_{pv}} \quad (11)$$

$$\frac{dP_{pv}}{dV_{pv}} = I_{pv}\frac{dV_{pv}}{dV_{pv}} + V_{pv}\frac{dI_{pv}}{dV_{pv}} \quad (12)$$

$$\frac{dP_{pv}}{dV_{pv}} = I_{pv} + V_{pv}\frac{dI_{pv}}{dV_{pv}} \quad (13)$$

Typically, the voltage generated by a source is positive. This algorithm's main goal is to identify the operating point of voltage where conductance matches the INC. Equations 14 – 16 conveys these principles and are visually represented in Figure 6. INC algorithm relies on P–V curve's slope, which is 0 at the MPP, rising at left of the MPP, and falling at right of the MPP. Equations 14 to 16 of the algorithm are outlined below:

$$\frac{dP}{dV} > 0 \text{ (The MPP's left side)} \quad (14)$$

$$\frac{dP}{dV} = 0 \text{ (MPP)} \quad (15)$$

$$\frac{dP}{dV} < 0 \text{ (The MPP's right side)} \quad (16)$$

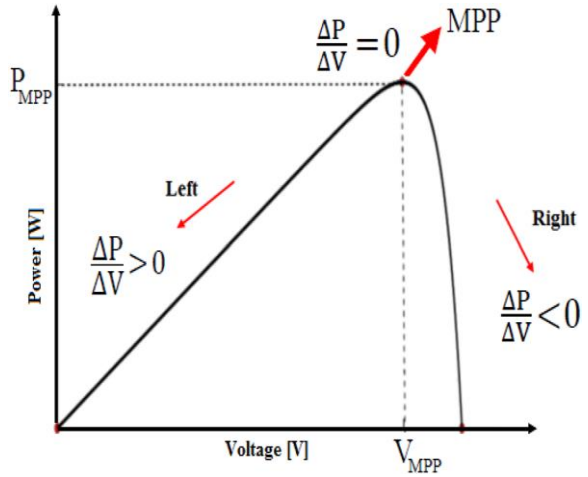

Figure 6: Solar Panel Performance Showcasing the MPP and Operational Principles [21]

The INC algorithm is developed by differentiating the output power of the PV module with respect to voltage and equating the result to zero. As a result, the connection between the instantaneous conductance (I/V) and the INC (ΔI/ΔV), as outlined in equations 17 – 19 can be established using Equation 10 in the following manner:

$$\frac{dI_{pv}}{dV_{pv}} = -\frac{I_{pv}}{V_{pv}} \quad \text{The MPP} \quad (17)$$

$$\frac{dI_{pv}}{dV_{pv}} > -\frac{I_{pv}}{V_{pv}} \quad \text{The MPP's left side} \quad (18)$$

$$\frac{dI_{pv}}{dV_{pv}} < -\frac{I_{pv}}{V_{pv}} \quad \text{The MPP's right side} \quad (19)$$

2.4 MPCC of the converter

MPC is a robust control methodology employed for anticipating system behavior by considering various control states. It proceeds by selecting the optimal control action for the next step based on predicted future system states, aiming to minimize a predefined cost function. The determination of this cost function at each sampling interval is influenced by the chosen prediction horizon (N), which can be tailored according to the system's characteristics and performance criteria. When the prediction horizon extends beyond one step, the predictions are iteratively shifted forward, and subsequent optimizations are conducted [19].

In this work, a prediction horizon of one (N = 1) is employed to identify the optimal next switching state. Consequently, a cost function incorporating future states, references, and forthcoming actions can be expressed as in equation 20 [19].

$$g = f\big(x(k), u(k), \dots\dots, u(k+N-1)\big) \quad (20)$$

To derive the discrete-time model, various discretization techniques are employed. One widely adopted method, as outlined in equation 21, is the forward-difference Euler approximation, particularly effective for first-order systems [12].

$$\frac{dV_L}{dt} \approx \frac{V_L(k+1)-V_L(k)}{T_S} \quad (21)$$

By combining equations 8 and 21, equation 22 is formulated to predict the subsequent inductor voltage value

$$V_L(k+1) = V_L(k) - \left(\frac{T_S R_L}{L}\right)\big(V_{in}(k) - I_L R_L(k) - V_{out}(k)(1-d)\big) \quad (22)$$

Where k is iteration number, T_s is time of sampling and $V_L(k+1)$ is predicted voltage value

At every instance of sampling, the optimization task described in equation 22 is readdressed, employing freshly acquired data to ascertain the updated status of the switch.

The MPC approach cannot solely ascertain the optimal key state through predictions alone. It necessitates minimizing the disparity between the reference and predicted values, achieved through the cost function outlined in the preceding third step. Hence, the significance of the cost function becomes evident as a fundamental aspect of MPC-based applications. Equation 23 is employed as the cost function. To establish this function within the MPC framework, the error between the reference value and the predicted value is computed as demonstrated by the equation 23.

$$g_i(k+1) = \big[V_{ref} - V_L(k+1)\big]^2 \quad (23)$$

The fixed-step control method, which predicts the subsequent value during each sampling interval, requires an additional cost function to reduce the frequency of switching [23]. Given that digital control techniques do not rely on comparators for generating the switching signal, they might exhibit varying switching frequencies. If the switching frequency closely matches the sampling frequency, the control error tends to rise. In order to reduce the switching frequency. Equation 24 employs a cost function, incorporating a weighting factor (λ) to mitigate its impact on the overall cost function. In this research, the weighting factor is set at 0.1 following the cost function classification method introduced by [12]

$$g_{sw}(k+1) = \lambda^*[d(k) - d(k-1)]^2 \quad (24)$$

To effectively manage both current and switching frequency simultaneously, as previously noted, two distinct cost functions are required. One notable advantage of the MPC method is its ability to regulate multiple parameters within a unified function. Hence, equation 25 constitutes a comprehensive cost function, by combining equations 23 and 24. Adopting the squared error technique across multiple term cost functions has been shown to yield superior outcomes, as documented by [20]. Consequently, this study opts for the same method to enhance result accuracy, thus justifying the utilization of the squares of equations 23 and 25.

$$g(k+1) = g_i(k+1) + g_{sw}(k+1) \quad (25)$$

The total cost function is computed at every sampling interval for all feasible switching states and subsequently minimized, as outlined in equation 26. Employing Equation 27, the value of $d(k)$ yielding the lowest cost function value is determined, leading to the selection of the switching state based on this procedure.

$$d(k) = [1\ 0] argmin_d g \quad (26)$$

$$min\, g(k+1) = min(g_i(k+1) + g_{sw}(k+1))(27)$$

3. Model predictive based MPP tracking control

MPPT algorithms identify the MPP by monitoring power parameters. A typical PV array characteristic is illustrated in Figure 7 and Figure 8. As depicted in the Figure 7, the MPP corresponds to the point where P= 409W. Likewise, the MPP can also be determined from the IV characteristics shown in figure 8. Figure 9 depicts the comprehensive flowchart of the proposed control structure. As illustrated in Figure 9, the control process initiates with the measurement of power parameters. Adjustments to the reference value are established by comparing the preceding and subsequent power parameters. After completing this procedure, the MPC algorithm initiates by establishing certain parameters, including passive component characteristics, potential switching state matrices, and the sampling time. In the sampling phase, both the prediction algorithm as per equation 22 and the cost function as per equation 27 are computed across all potential switching states. The switch position is selected based on the smaller cost function, resulting in the MPC algorithm executing current control according to the MPPT reference.

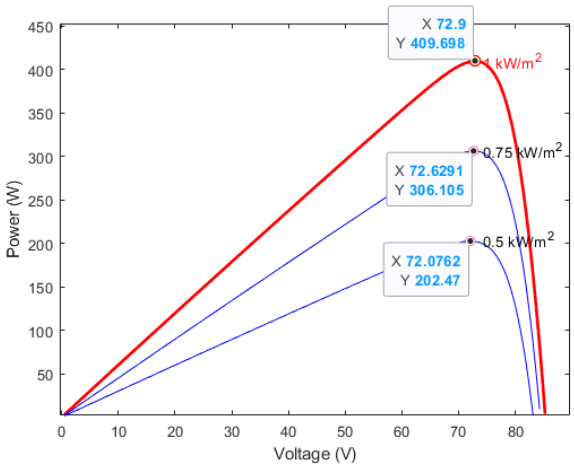

Figure 7: P-V Characteristics Plot

4. Result and Discussion

4.1 Steady Irradiance and Temperature

Figure 10 shows the variation of temperature with time while Figure 11 shows the variation of irradiance with time. It can be seen from Figure 10 that the value of temperature is 25˚C and remains unchanged from 0 to 1s, it then increased to 35˚C from 1s to 2s and then decreased to 25˚C from 2s to 3s. Also, the value of irradiance from figure 11 is 1000W/m^2 and remains constant from 0 to 3s.

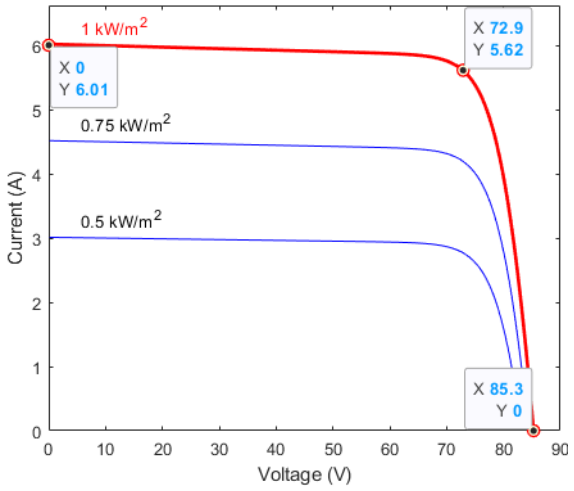

Figure 8: I-V Characteristics Plot

4.2 PO-MPC method for steady irradiance and changing temperature

Figure 12 shows power- time plot, Figure 13 shows current-time plot while Figure 14 shows voltage-time plot of PO-MPC method under steady irradiance and changing temperature. From Figure 12, at temperature 25˚C, the PO-MPC tracked the power to be 395.1W at 0.23s as compared to 410W of the PV power of the system at constant irradiance. Therefore, with PO-MPC method, the efficiency is found to be 96.3% with a tracking error of 3.7%. When the temperature was increased to 35˚C, the PO-MPC tracked the power to be 396.9W at time 1s as compared to 410W of the PV power of the system.

The efficiency at that period is found to be 96.8% with a tracking error of 3.2%. Also, when the temperature was decreased to 25˚C, the PO-MPC tracked the power to be 395.9W at 2.32s as compared to 410W of the PV power of the system. Therefore, the efficiency is found to be 96.5% with a tracking error of 3.5%.

Furthermore, Figure 13 and Figure 14 shows the voltage and current plots. At 25˚C, the voltage at the MPPis found to be 62.52V, when the temperature was increased to 35˚C, the voltage at the MPPis found to be 62.76V and 62.70V when the temperature decreased to 25˚C. Similarly, at 25˚C, the current at MPPis found to be 6.33A, 6.33A at 35˚C, and 6.32A when the temperature was reduced to 25˚C.

4.3 Steady Irradiance and changing Temperature for INC-MPC

Figure 15 shows power- time plot, Figure 16 shows current-time plot while Figure 17 shows voltage-time plot of INC-MPC method under steady irradiance and changing temperature. From Figure 15, at temperature 25˚C, the INC-MPC tracked the power to be 403W at 0.24s as compared to 410W of the PV power of the system. Therefore, with the INC-MPC, the efficiency is found to be 98.2% with a tracking error of 1.8%. Also, the power tracked by the INC-MPC at 35˚C is found to be 405.4W at 1s as compared to 410W of the PV power of the system.

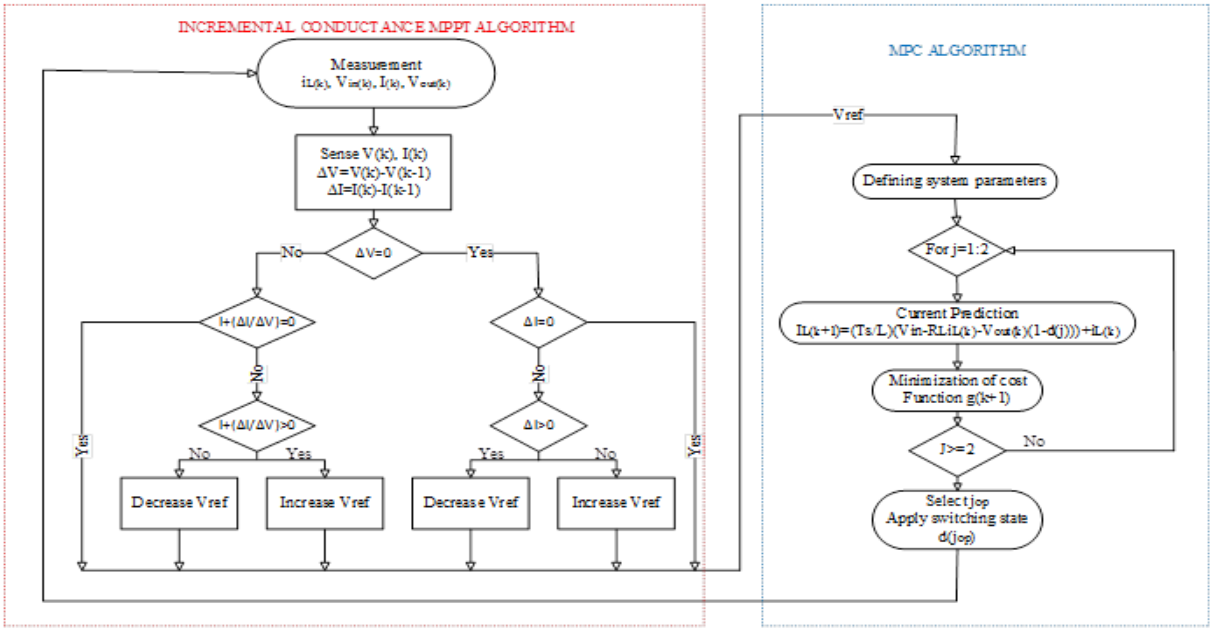

Figure 9: Flow-Chart of INC-MPC Based MPPT

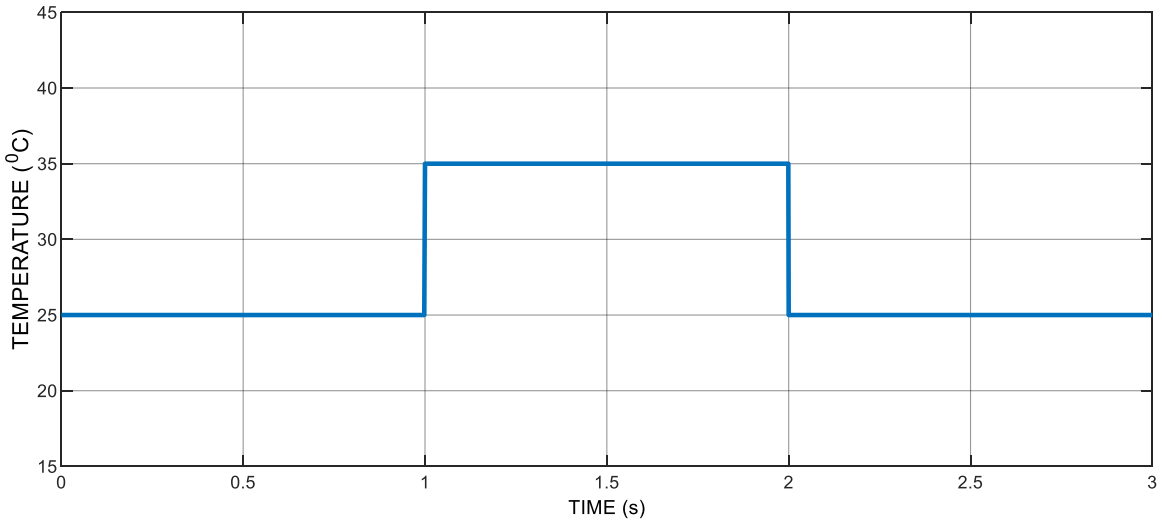

Figure 10: Temperature – Time Plot

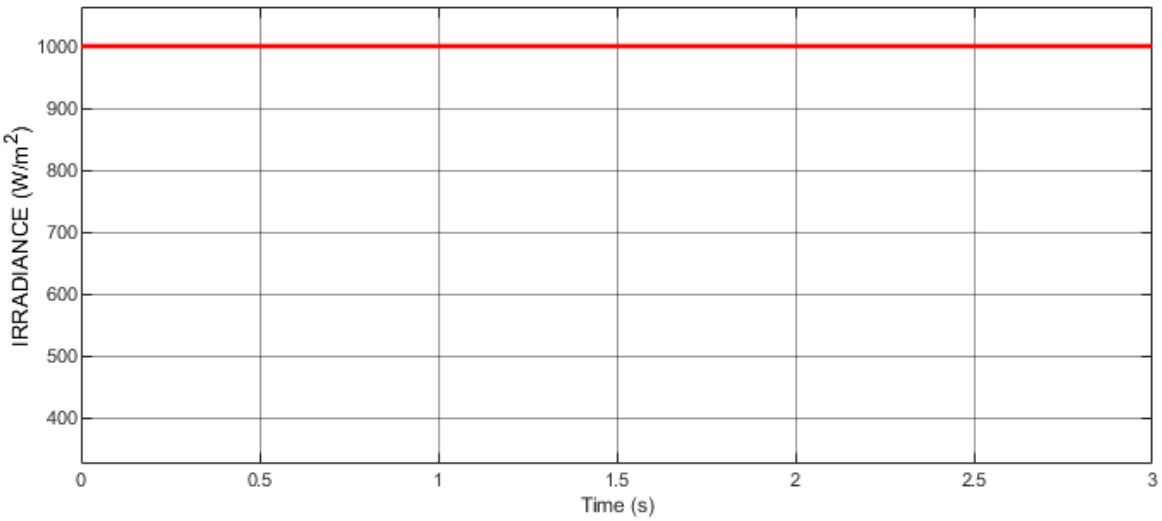

Figure 11: Irradiance – Time Plot

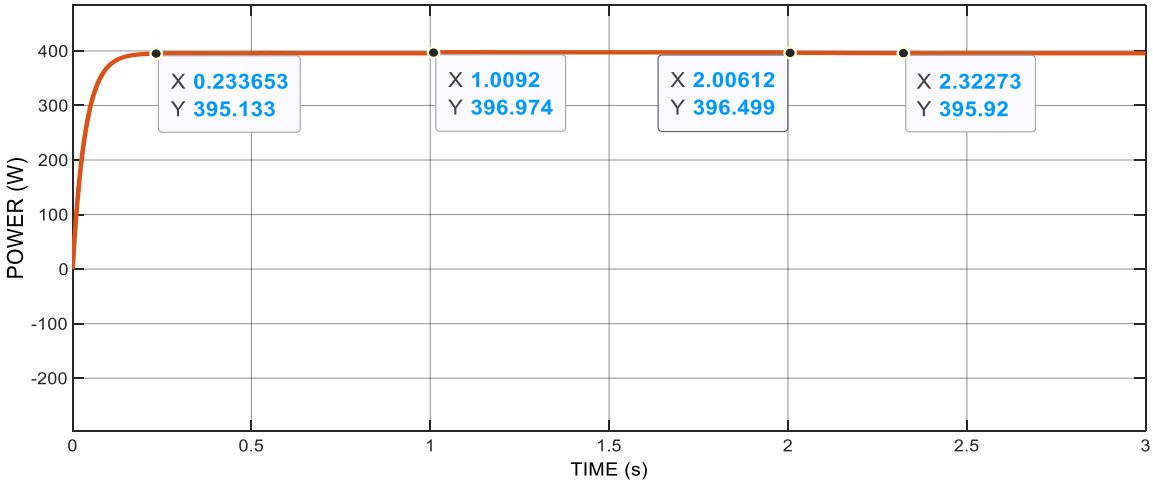

Figure 12: Power – Time Plot of PO –MPC Method

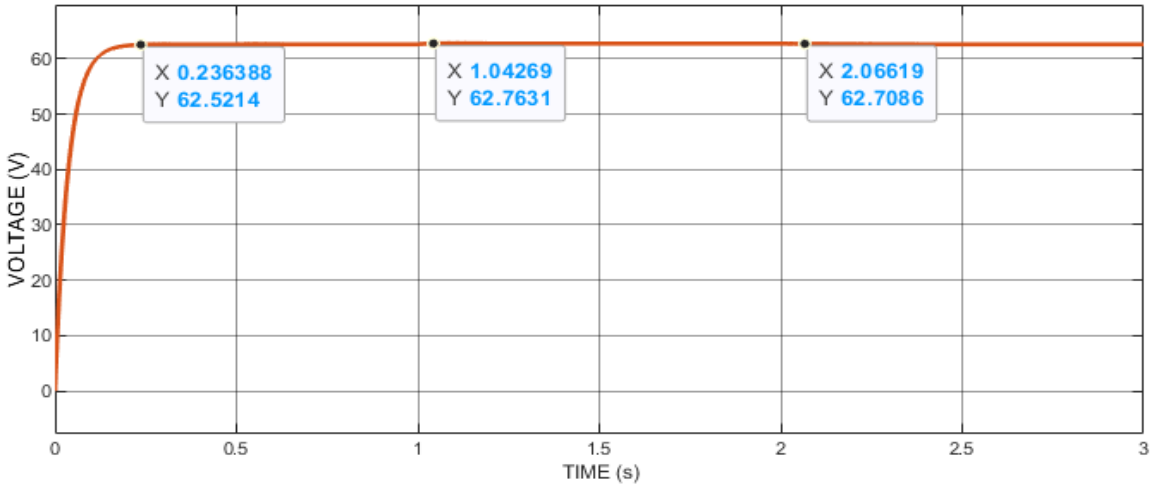

Figure 13: Voltage – Time Plot of PO-MPC

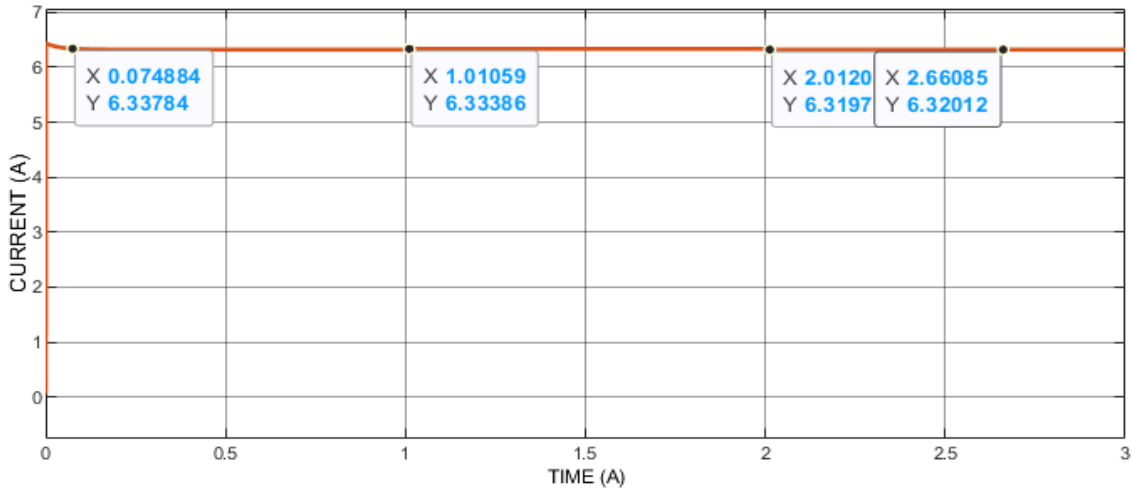

Figure 14: Current – Time Plot of PO-MPC Method

Therefore, the efficiency is found to be 98.8% with a tracking error of 1.2%. At 25˚C, the INC-MPC then tracked the power to be 403.9W at 2.1s as compared to 410W of the PV power of the system. At this point, the efficiency is found to be 98.5% with a tracking error of 1.5%. Furthermore, Figure 16 and Figure 17 shows voltage and current plots. Voltage at MPPis found to be 63.19V at 25˚C, 63.3V at 35˚C and 63.3V at 25˚C. Similarly, at 25˚C, the current at MPPis found to be 6.4A, when the temperature was increased to 35˚C, current at the MPPis found to be 6.4A and 6.38A at 25˚C.

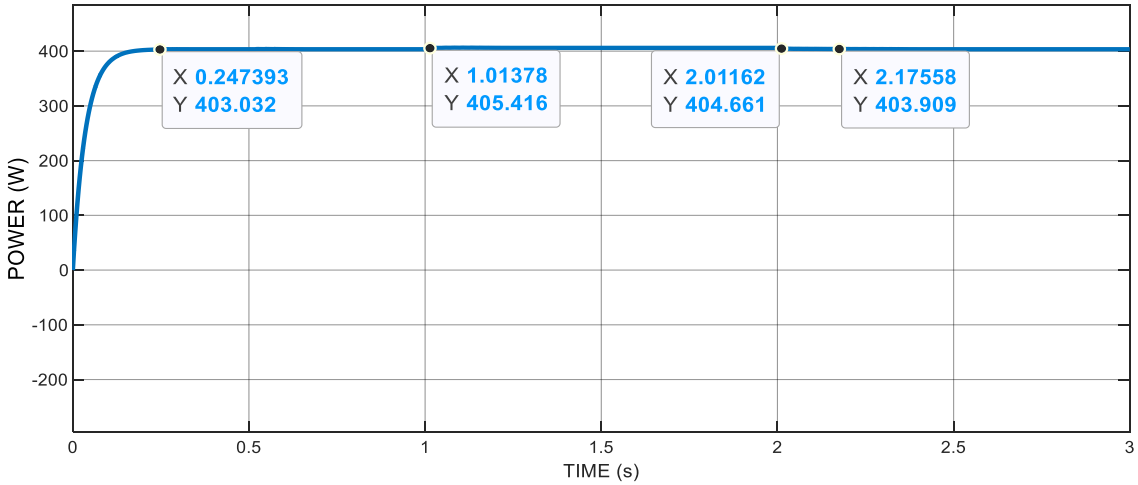

Figure 15: Power –Time Plot of INC-MPC Method

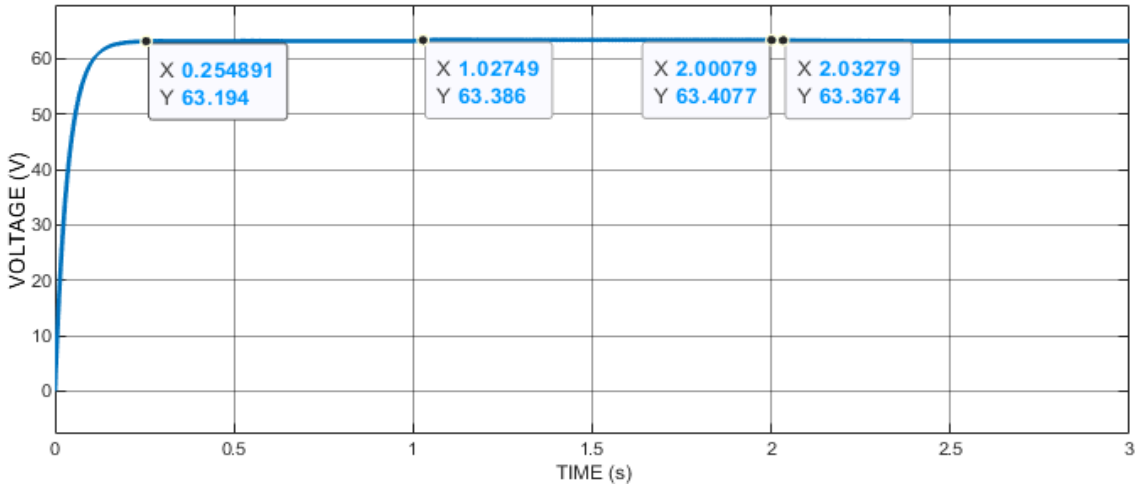

Figure 16: Voltage – Time Plot of INC-MPC Method

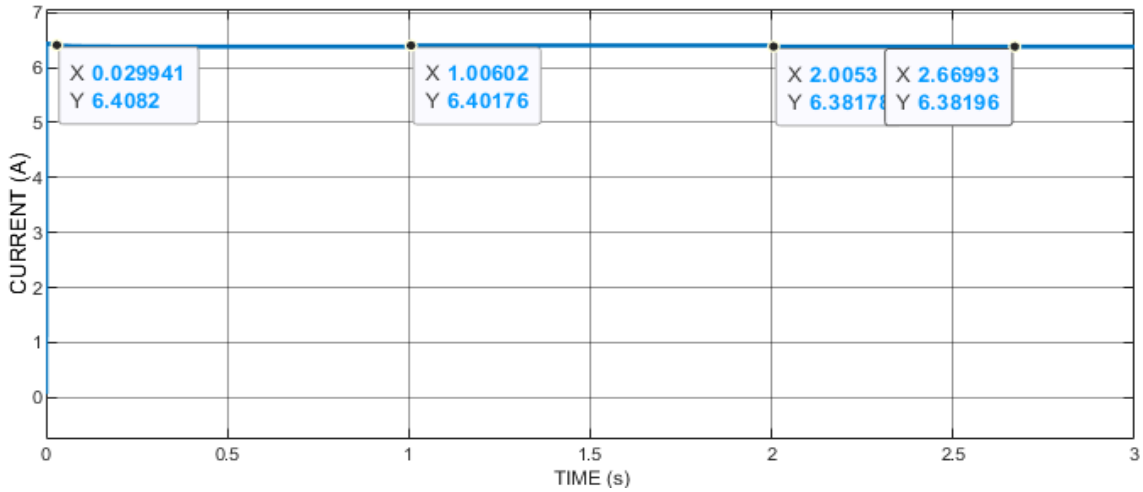

Figure 17: Current – Time Plot of INC-MPC Method

4.4 Comparison of PO-MPC and INC-MPC method

Table 1 shows the comparison between PO-MPC and INC-MPC in terms of tracking time and relative error. Under constant irradiance and variable temperature condition, the results of the developed method and PO-MPC method were compared and the results are shown in Table 1. From the comparison Table 1, it was established that the INC-MPC have a shorter tracking time and lower relative error compared to PO-MPC method. This indicates that INC-MPC is more responsive and can adapt to changes faster than PO-MPC method.

Table 1: Results obtained from the developed method and Irmark and Guler [6] at Varying Temperature and Constant Irradiance

Parameter Description	PO-MPC	Developed method	% Reduction
Tracking Time at 25^{0}C (sec)	0.23	0.22	4.3
Tracking Time at 35^{0}C (sec)	1.01	1.00	0.99
Tracking Time at 25^{0}C (sec)	2.32	2.1	9.5
Relative error at 25^{0}C (%)	3.7	1.8	1.9
Relative error at 35^{0}C (%)	3.2	1.2	2
Relative error at 25^{0}C (%)	3.5	1.5	2

Table 2 shows the comparison of PO-MPC method and INC-MPC method in terms of efficiency. The table displays the efficiency percentages for both methods and showing that the INC-MPC outperformed the PO-MPC method in terms of efficiency. The data indicates that INC-MPC is more effective in optimizing the maximum power tracking technique.

Table 2: Efficiency under Varying Temperature and Constant Irradiance

Parameter Description	PO-MPC	INC-MPC	% Improvement
Efficiency at 25^{0}C (%)	96.3	98.2	1.9
Efficiency at 35^{0}C (%)	96.8	98	1.2
Efficiency at 25^{0}C (%)	96.5	98.5	2

5. Conclusion

Various techniques, algorithms, and methods have been developed and applied for tracking the MPP to optimize the performance of PV (PV) systems. Selecting an appropriate MPPT technique necessitates careful evaluation of factors such as cost, reliability, speed, accuracy, and efficiency. Moreover, the power ratings of the PV panels and the local climate conditions are crucial considerations in certain areas and applications. All components required for modeling and simulating the INC-MPC MPPT control method were thoroughly detailed and modeled, along with an explanation of their operation. The system was then simulated using MATLAB/Simulink, and the resulting simulations were presented and discussed. The results demonstrated that the INC-MPC method perform well above PO-MPC methods in terms of dynamic respond and efficiency. Furthermore, it exhibits almost zero oscillation at a steady state, leading to significant power savings.

References

[1]. Gevorkian, P., (2011). *Large-Scale Solar Power System Design (GreenSource Books): An Engineering Guide for Grid-Connected Solar Power Generation*, McGraw Hill Professional, New York.

[2]. Farret, A. F. and Godoy, M. S., (2006). *Integration of Alternative Sources of Energy*, John Willey and Sons Inc, New Jersey.

[3]. Maka, A. O. and Alabid, J. M., (2022). Solar energy technology and its roles in sustainable development. *Clean Energy, 6*(3), 476-483. https://doi.org/10.1093/ce/cdz036

[4]. Irmak, E. and Güler, N., (2020). A model predictive control-based hybrid MPPT method for boost converters, *International Journal of Electronics, 107*(1), 1-16. https://doi.org/10.1080/00207217.2019.1678238

[5]. Baba, A. O., Liu, G. and Chen, X., (2020). Classification and evaluation review of maximum power point tracking methods, *Sustainable Futures*, *2*, 100020.

[6]. Kandemir, E., Borekci, S. and Cetin, N. S., (2018). Comparative analysis of reduced-rule compressed fuzzy logic control and INC MPPT methods, *Journal of Electronic Materials, 47*, 4463-4474. https://doi.org/10.1007/s11664-018-6321-2.

[7]. Khosravi, M., Heshmatian, S., Khaburi, D. A., Garcia, C. and Rodriguez, J., (2017). *A novel hybrid model-based MPPT algorithm based on artificial neural networks for photovoltaic applications,* In *2017 IEEE Southern Power Electronics Conference (SPEC),* April, 2017, Chile (pp. 1-6). IEEE. https://doi.org/10.1109/SPEC.2017.8305446

[8]. Kim, S. K., Park, C. R., Kim, J. S. and Lee, Y. I., (2014). A stabilizing model predictive controller for voltage regulation of a DC/DC boost converter, *IEEE Transactions on Control Systems Technology, 22*(5), 2016-2023. https://doi.org/10.1109/TCST.2013.2287314

[9]. Mahendran, V. and Ramabadran, R., (2016). Fuzzy-PI-based centralised control of semi-isolated FP-SEPIC/ZETA BDC in a PV/battery hybrid system, *International Journal of Electronics, 103*(11), 1909–1927.

[10]. Öztürk, N. and Çelik, E., (2014). An educational tool for the genetic algorithm-based fuzzy logic controller of a permanent magnet synchronous motor drive, *International Journal of Electrical Engineering Education, 51*(3), 218-231. https://doi.org/10.1177/0020720914540411

[11]. Singh, S., Fulwani, D. and Kumar, V., (2017). Emulating DC constant power load: A robust sliding mode control approach, *International Journal of Electronics, 104*(9), 1447-1464. https://doi.org/10.1080/00207217.2016.1250001

[12]. Rodriguez, J. and Cortes, P., (2012). *Predictive control of power converters and electrical drives*, John Wiley and Sons, New Jersey.

[13]. Seo, S. W., Kim, Y. and Choi, H. H., (2017). Model predictive controller design for boost DC–DC converter using T–S fuzzy cost function, *International Journal of Electronics, 104*(11), 1838-1853. https://doi.org/10.1080/00207217.2017.1341991

[14]. Cheng, L., Acuna, P., Aguilera, R. P., Ciobotaru, M. and Jiang, J., (2016). *Model predictive control for DC-DC boost converters with constant switching frequency*, In *2016 IEEE 2nd Annual Southern Power Electronics Conference (SPEC), December, 2016,* Auckland, pp. 1-6, IEEE.

[15]. Ren, H. P., Zheng, M. M. and Li, J., (2015). *A simplified mixed logical dynamic model and model*

predictive control of boost converter with current reference compensator, In *2015 IEEE 24th International Symposium on Industrial Electronics (ISIE),* October, 2015, Brazil, pp. 61-65. IEEE. https://doi.org/10.1109/ISIE.2015.7281406

[16]. Lashab, A., Sera, D., Guerrero, J. M., Mathe, L. and Bouzid, A., (2017). Discrete model-predictive-control-based maximum power point tracking for PV systems: Overview and evaluation, *IEEE Transactions on Power Electronics, 33*(8), 7273-7287. https://doi.org/10.1109/TPEL.2017.2682698

[17]. Adhikari, N., (2018). Design of solar photovoltaic energy generation system for off-grid applications, *International Journal of Renewable Energy Technology, 9*(1-2), 198-207. https://doi.org/10.1504/IJRET.2018.091589

[18]. Priya, T. H. and Parimi, A. M., (2016). *Design of adaptive perturb and observe-fuzzy MPPT controller for high voltage gain multilevel boost converter*, In *2016 IEEE 7th Power India International Conference (PIICON), November, 2016, Bikaner,* pp. 1-6. IEEE.

[19]. Metry, M., Bayhan, S., Shadmand, M. B., Balog, R. S. and Rub, H. A., (2016). *Sensorless current model predictive control for maximum power point tracking of single-phase subMultilevel inverter for photovoltaic systems*, In *2016 IEEE Energy Conversion Congress and Exposition (ECCE),* February, 2016, Illinois, pp. 1-8. IEEE. https://doi.org/10.1109/ECCE.2016.7855120

[20]. Mosa, M., Shadmand, M. B., Balog, R. S. and Abu Rub, H., (2017). Efficient maximum power point tracking using model predictive control for photovoltaic systems under dynamic weather condition, *IET Renewable Power Generation, 11*(11), 1401-1409. https://doi.org/10.1049/iet-rpg.2016.0970

[21]. Mohamed, S. A. and Abd El Sattar, M., (2019). A comparative study of P and O and INC maximum power point tracking techniques for grid-connected PV systems, *SN Applied Sciences, 1*(2), 174. https://doi.org/10.1007/s42452-019-0191-4

[22]. Moghassemi, A., Ebrahimi, S. and Olamaei, J., (2020). Maximum power point tracking methods used in photovoltaic systems: A review, *Signal Processing and Renewable Energy, 4*(3), 19-39. https://doi.org/10.38064/spre.v4i3.256

[23]. Danandeh, M. A. and Mousavi, S. M. G., (2018). Comparative and comprehensive review of maximum power point, *Renewable and Sustainable Energy Reviews*, 82(3), 2743–2767.